



Comprehensive Analysis of Ferroptosis- and Immune-Related Signatures to Improve the Prognosis and Diagnosis of Kidney Renal Clear Cell Carcinoma

OPEN ACCESS

Edited by:

Hailin Tang,
Sun Yat-sen University Cancer Center
(SYSUCC), China

Reviewed by:

Yong Yang,
China Pharmaceutical
University, China
Qianjin Liao,
Central South University, China

*Correspondence:

Yan Zhou
921lan@sina.com
Zhiqian Xiao
xzq1892000@163.com

Specialty section:

This article was submitted to
Cancer Immunity
and Immunotherapy,
a section of the journal
Frontiers in Immunology

Received: 09 January 2022

Accepted: 12 April 2022

Published: 10 May 2022

Citation:

Xing X-L, Liu Y, Liu J, Zhou H,
Zhang H, Zuo Q, Bu P, Duan T, Zhou Y
and Xiao Z (2022) Comprehensive
Analysis of Ferroptosis- and Immune-
Related Signatures to Improve the
Prognosis and Diagnosis of Kidney
Renal Clear Cell Carcinoma.
Front. Immunol. 13:851312.
doi: 10.3389/fimmu.2022.851312

Xiao-Liang Xing^{1,2}, Yan Liu¹, Jiheng Liu³, Huanfa Zhou¹, Huirong Zhang¹, Qi Zuo³,
Ping Bu¹, Tong Duan³, Yan Zhou^{3*} and Zhiqian Xiao^{1*}

¹ Department of General Medicine, University of South China affiliated Changsha Central Hospital, Changsha, China, ² School of Public Health and Laboratory Medicine, Hunan University of Medicine, Huaihua, China, ³ Department of Emergency, First Hospital of Changsha, Changsha, China

Background: Almost 40% of patients with kidney renal clear cell carcinoma (KIRC) with advanced cancers eventually develop to metastases, and their 5-year survival rates are approximately 10%. Aberrant DNA methylations are significantly associated with the development of KIRC. The aim of our present study was to identify suitable ferroptosis- and immune-related (FI) biomarkers correlated with aberrant methylations to improve the prognosis and diagnosis of KIRC.

Methods: ChAMP and DESeq2 in R (3.6.2) were used to screen the differentially expressed methylation probes and differentially expressed genes, respectively. Univariate and multivariate Cox regression were used to identify the overall survival (OS)-related biomarkers.

Results: We finally identified five FI biomarkers (*CCR4*, *CMTM3*, *IFITM1*, *MX2*, and *NR3C2*) that were independently correlated with the OS of KIRC. The area under the curve value of the receiver operating characteristic value of prognosis model was 0.74, 0.68, and 0.72 in the training, validation, and entire cohorts, respectively. The sensitivity and specificity of the diagnosis model were 0.8698 and 0.9722, respectively. In addition, the prognosis model was also significantly correlated with several immune cells and factors.

Conclusion: Our present study suggested that these five FI-DEGs (*CCR4*, *CMTM3*, *IFITM1*, *MX2*, and *NR3C2*) could be used as prognosis and diagnosis biomarkers for patients with KIRC, but further cross-validation clinical studies are still needed to confirm them.

Keywords: KIRC, methylation, ferroptosis, immune, prognosis, diagnosis

INTRODUCTION

Kidney cancer is the second most common malignancies in the urinary system, which accounts for 2.2% of all new cancer cases, with over 430,000 new cases and 1.8% of all cancer related death, with almost 180,000 deaths in 2020 globally (1). Kidney renal clear cell carcinoma (KIRC) is the most common subtype, which accounts for 75% of kidney cell carcinomas (2, 3). Surgery is the primary treatment for KIRC (4, 5). However, almost 40% of patients with KIRC with advanced cancers eventually develop to metastases despite of early surgical treatment carried out (6, 7). Patients with KIRC have poor prognosis and high mortality rates, and their 5-year survival rates are approximately 10% (3, 8). Therefore, it is very necessary to identify potential prognosis biomarkers for the diagnosis and prognosis of KIRC.

Epigenetics was originally coined by Conrad Waddington, which plays a critical role in the regulation of DNA-based processes (9). Consequently, abnormal expression patterns or genomic alterations caused by abnormal epigenetic modifications may induce and maintenance various cancers (9). Accumulating pieces of evidence indicate that epigenetic alterations are the early events of cancerigenesis (9–11). For example, several key cancerigenesis related pathways could be regulated by epigenetic, such as Wnt/ β -catenin signaling pathway, Hedgehog signaling pathway, and Notch signaling pathway (12–14). DNA methylations as the typical epigenetic manners are indeed involved in procession of many cancer stem cells, such as leukemic, lung and colon stem cells (15–17). In addition, previous studies have also demonstrated that aberrant DNA methylations are significantly correlated with the procession of KIRC (18, 19).

Numerous studies demonstrated that ferroptosis and immune can regulate each other and participate in the progression of several cancers (20–25). Regulation of ferroptosis and immune are currently considered to be novel therapeutic targets for the cancers (24, 26–29). The Cancer Genome Atlas (TCGA) is an open access database. In the present study, we downloaded 484 methylation data, 602 RNA sequencing (RNA-seq) data and the corresponding clinical information from TCGA and aimed to identify suitable ferroptosis- and immune-related (FI) biomarkers correlated with aberrant methylations to improve the prognosis and diagnosis of KIRC.

MATERIALS AND METHODS

Data Source and Data Processing

The data used in present study were obtained from an open access database TCGA, including 484 samples (160 controls vs. 324 cancers) of methylation data, 602 samples (72 controls vs. 530 cancers) of RNA-seq data, and the corresponding clinical information. The recognized FI-related genes were obtained from the FerrDb and ImmPort, respectively. We used ChAMP and DESeq2 in R (3.6.2) to screen the differentially expressed methylatyon probes (DMPs) as the criteria $\text{padj} < 0.05$ and $|\log\text{FC}| \geq 0.2$ and differentially expressed genes (DEGs) as the

criteria $\text{padj} < 0.05$ $|\log\text{FC}| \geq 0.5$ and base mean ≥ 100 , respectively. Pearson correlation analyses were used to determine the relationship of DEGs and their corresponding DMPs as the criteria $R \leq -0.3$. To construct a prognostic model and verify it, 530 patients with KIRC were randomly separated into training ($n = 354$) and validation ($n = 176$) cohorts (Table 1).

Construction of Prognosis and Diagnostic Model

We divided the patients with KIRC into low-expression cohort and high-expression cohort by the median expression value. The univariate Cox regression and multivariate Cox regression in R (3.6.2) were used to identify the candidate biomarkers. After multivariate Cox hazards regression, we constructed the prognostic model according to the previous reports (30, 31). Risk score = $(-0.9653) \times \text{Exp}_{(\text{CCR4})} + (-0.7026) \times \text{Exp}_{(\text{CMTM3})} + (0.8370) \times \text{Exp}_{(\text{IFITM1})} + (0.8450) \times \text{Exp}_{(\text{MX2})} + (-0.7717) \times \text{Exp}_{(\text{NR3C2})}$

Patients with KIRC were divided into low-risk cohort and high-risk cohort depends on the optimal cutoff value (Youden Index).

After a stepwise logistic regression analyses, the diagnostic model was constructed as follows: LOGIT score = $0.7998 + (0.1034) \times \text{Exp}_{(\text{CMTM3})} + (-0.1590) \times \text{Exp}_{(\text{NR3C2})} + (0.0465) \times \text{Exp}_{(\text{MX2})} + (0.0737) \times \text{Exp}_{(\text{CCR4})} + (0.0966) \times \text{Exp}_{(\text{IFITM1})}$

Enrichment Analyses and Principal Component Analyses

David 6.8 was used to carry out Gene Ontology (GO) and Kyoto Encyclopedia of Genes and Genomes (KEGG) enrichment analyses with the default parameter (<https://david.ncifcrf.gov/>). A principal component analyses (PCAs) in R (3.6.2) was used to reduce the dimensions and to visualize the distribution of the patients with KIRC.

Statistical Methods

A repeated-measure ANOVA followed by Bonferroni *post hoc* tests or unpaired two-tail Student's t-test was used as indicated.

RESULTS

Identification of Candidate Prognostic Biomarkers

We downloaded methylation data of 484 samples (160 controls vs. 324 cancers) from the TCGA database and obtained 15,025 DMPs by ChAMP. Of which, 9,294 were hypermethylated DMPs and 5,731 were hypomethylated DMPs (Figure 1A). The distributions of those 15,025 DMPs were showed in Figure 1B by considering the CpG content and the neighboring context.

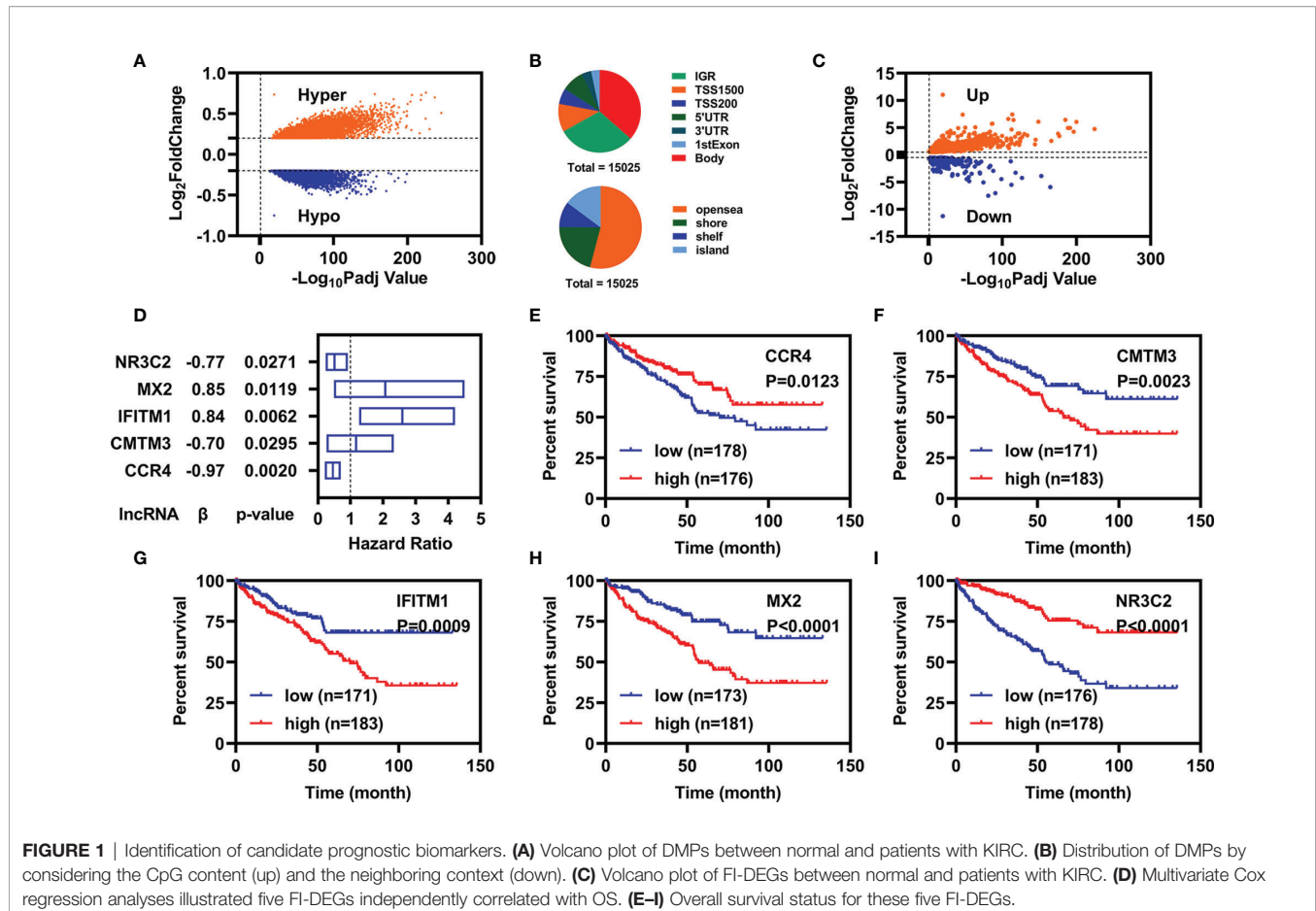
Similarly, we also downloaded RNA-seq data of 602 samples (72 controls vs. 530 cancers) from TCGA database and obtained 7,500 DEGs (4,515 were upregulated DEGs and 2,985 were downregulated DEGs) through DESeq2 (Supplementary Figure 1). Of which, there were 784 DEGs were FI-DEGs

TABLE 1 | Clinical features of patients in the training cohort and validation cohort.

Variables		Training Cohort (n = 354)		Validation Cohort (n = 176)	
		No.	%	No.	%
Age	≤65	229	64.69	119	67.61
	>65	125	35.31	57	32.39
Stage	I	183	51.69	82	46.59
	II	34	9.60	23	13.07
	III	84	23.73	39	22.16
	IV	52	14.69	30	17.05
T	X	1	0.28	2	1.14
	T1	187	52.82	84	47.73
	T2	40	11.30	29	16.48
	T3	120	33.90	59	33.52
N	T4	7	1.98	4	2.27
	N0	165	46.61	74	42.05
	N1	9	2.54	7	3.98
M	NX	180	50.85	95	53.98
	M0	283	79.94	137	77.84
	M1	49	13.84	29	16.48
Gender	MX	22	6.21	10	5.68
	Female	131	37.01	55	31.25
	Male	223	62.99	121	68.75

(Figure 1C). Then, we introduced Pearson correlation analyses for those 15,025 DMPs and their corresponding FI-DEGs and found that there were 138 FI-DEGs correlated with 256 DMPs (Supplementary Table 1).

To obtain suitable FI-DEGs as biomarkers, we firstly performed the univariate Cox regression analyses for those 138 FI-DEGs correlated with DMPs and found 61 FI-DEGs were correlated with the overall survival (OS) of patients with KIRC in



the training cohort. We then performed the multivariate Cox regression analyses for those 61 FI-DEGs and found that five of 61 FI-DEGs (*CCR4*, *CMTM3*, *IFITM1*, *MX2*, and *NR3C2*) were independently correlated with the OS of patients with KIRC (**Figure 1D**). Kaplan–Meier (KM) curve showed patients with KIRC with high expression of *CCR4* and *NR3C2* displayed better OS, whereas patients with high expression of *CMTM3*, *IFITM1*, and *MX2* displayed worse OS (**Figures 1E–I**).

Specific Prognostic Model Construction

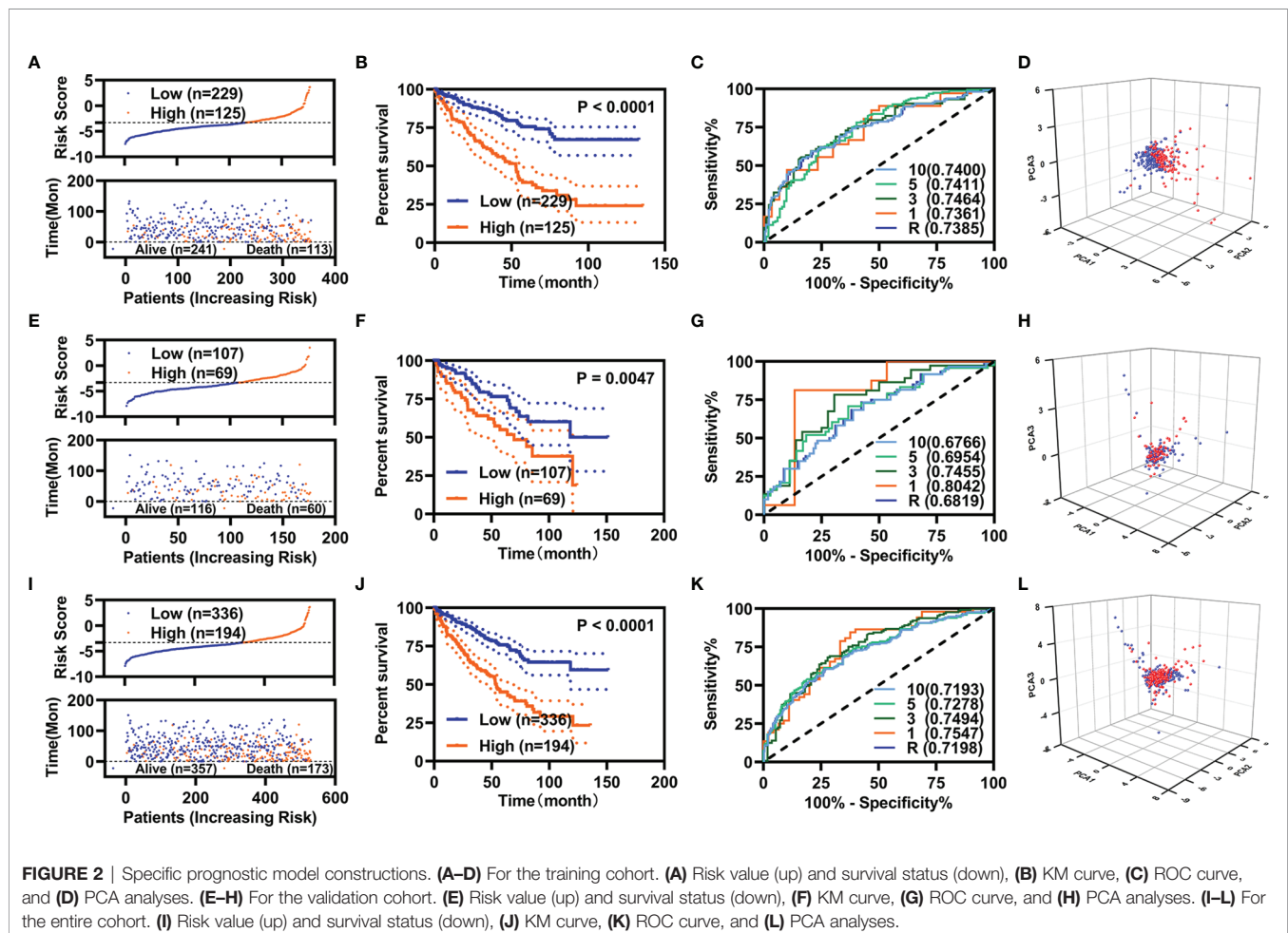
After multivariate Cox regression analyses, we constructed a specific prognostic model using those five FI-DEGs. Depending on the Youden Index as the optimal cutoff value (**Supplementary Figure 2**), we regrouped the patients with KIRC into low-risk cohort and high-risk cohort. The expressions of these five FI-DEGs between patients with KIRC with the low-risk cohort and high-risk cohort were displayed in **Supplementary Figures 3A–C**. The correlations of these five FI-DEGs with the risk value were displayed in **Supplementary Figures 3D–F**. *CCR4*, *IFITM1*, and *MX2* were significantly correlated with the prognostic model (**Supplementary Figures 3D–F**).

We constructed prognostic models using these five FI-DEGs in the training, validation, and entire cohort. In the training cohort, the

risk score (up) and survival status (down) for each patients with KIRC were displayed in **Figure 2A**. Patients with KIRC with low-risk value had longer survival time [**Figure 2A** (down)]. KM curve showed patients with KIRC with low-risk value displayed better OS (**Figure 2B**). The time dependent area under the curve (AUC) value of receiver operating characteristic (ROC) of the prognostic model was displayed in **Figure 2C**. All AUC values were over 0.70. The patients with high-risk value could well be distinguished from the whole patients as measured by the PCA analyses (**Figure 2D**). To determine whether these five biomarkers were feasible, we conducted validation studies in validation cohort and entire cohort. The similar results were displayed in **Figures 2E–L**. In all three cohorts, the 5-year AUC value of the prognostic model reached 0.70 (**Figures 2C, G, K**). These results indicated the prognostic model constructed using those five FI-DEGs could well predict the outcome of patients with KIRC.

Clinical Evaluation of the Prognostic Model

To know the role of the prognostic model in the prediction, we performed univariate and multivariate Cox regression analyses for the prognostic model and the variant clinical features. In the training cohort, the age, pathological TNM, pathologic stage, and



the prognostic model were correlated with the OS as measured by univariate Cox regression analyses (Figure 3A). The pathological M and prognostic model were independently correlated with the OS as measured by multivariate Cox regression analyses (Figure 3B). In addition, the AUC value of prognostic model was high than that of the pathological M (Figure 3C).

In the validation cohort, the age, pathological TNM, pathologic stage, and the prognostic model were correlated with the OS as measured by univariate Cox regression analyses (Figure 3D). The pathological M was independently correlated with the OS as measured by multivariate Cox regression analyses (Figure 3E). The AUC value of prognostic model was comparable with that of the pathological M (Figure 3F).

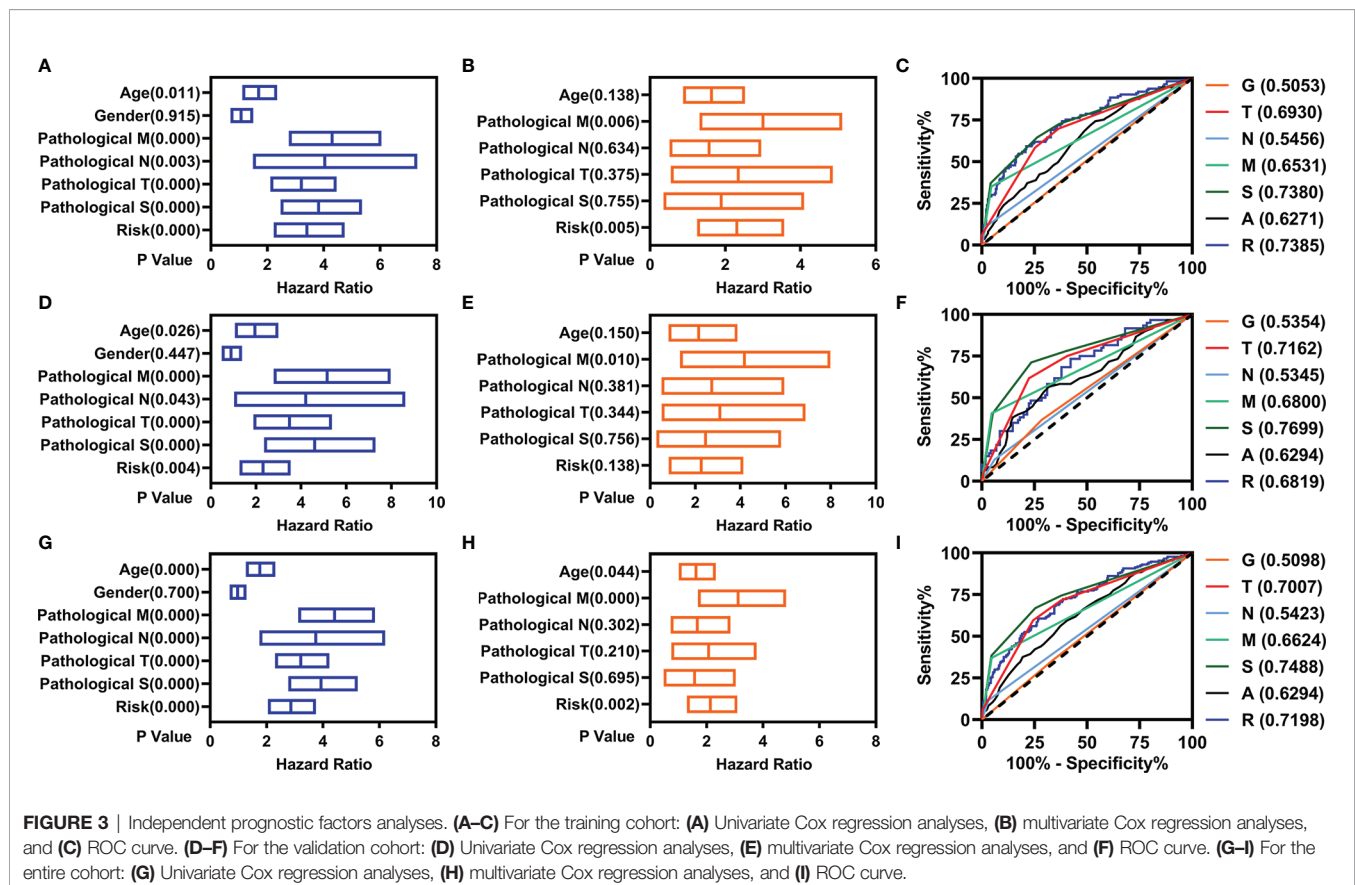
In the entire cohort, the age, pathological TNM, pathologic stage, and the prognostic model were correlated with the OS as measured by univariate Cox regression analyses (Figure 3G). The age, pathological M, and prognostic model were independently correlated with the OS as measured by multivariate Cox regression analyses (Figure 3H). The AUC value of prognostic model was higher than that of the age and pathological M (Figure 3I).

We also explored the relationship of the expression of these five FR-DEGs and the risk value with the clinical features. The results were displayed in Figure 4.

Correlation Analyses of the Prognostic Model With the Immunity

We evaluated the immunity status of the patients with KIRC using these 7,500 DEGs by ESTIMATE in R (3.6.2). The ESTIMATE score, immune score, and stromal score were significantly increased, whereas the tumor purity was significantly decreased in the patients with KIRC (Figures 5A–D). Moreover, the ESTIMATE score, immune score, and stromal score were significantly decreased, whereas the tumor purity was significantly increased in the patients with KIRC with high-risk value (Figures 5E–H). In addition, the expression of CCR4, MX2, and NR3C2 were significantly correlated with the stromal score, immune score, ESTIMATE score, and tumor purity (Figure 5I). IFITM1 expression was significantly correlated ESTIMATE score and tumor purity (Figure 5I).

We also evaluated the relationship of infiltration of immune cells and factors with the risk value. First, we found that there were 88 immune cells and factors whose infiltration values were significantly difference between normal and patients with KIRC (Supplementary Table 2). Of which, there were 53 immune cells and factors that are significantly difference between patients with KIRC with low-risk value and high-risk value (Figures 6A–G). Correlation analyses showed six immune cells and factors were significantly correlated with the risk value (Figure 6H). In addition, these five FI-DEGs were also significantly correlated



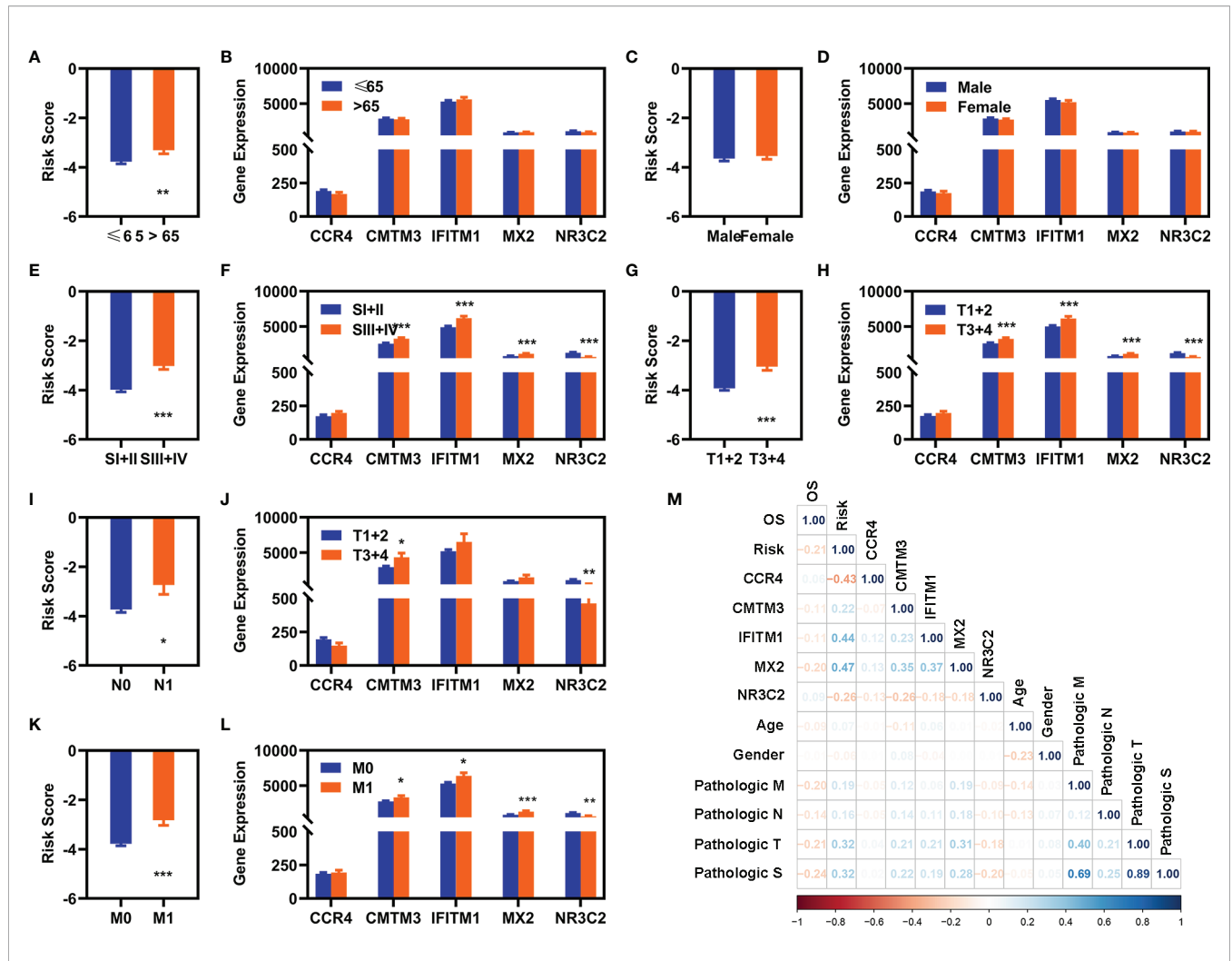


FIGURE 4 | Correlation analyses with clinical features. (A, C, E, G, I, K) Differentially expression analyses of risk value with clinical different features in the entire cohort [(A) age, (C) gender, (E) pathological S, (G) pathological T, (I) pathological (N), and (K) pathological (M)]. (B), (D), (F), (H), (J), (L) Differentially expression of these five FI-DEGs with clinical features in the entire cohort [(A) age, (C) gender, (E) pathological S, (G) pathological T, (I) pathological (N), and (K) pathological (M)]. (M) Correlation analyses of these five FI-DEGs and risk value with the clinical features in the entire cohort. N (≤ 65) = 348, N (>65) = 182. N (Male) = 344, N (Female) = 186. N (SI + II) = 322, N (III + IV) = 205. N (T1 + 2) = 340, N (T3 + 4) = 190. N (N0) = 239, N (N1) = 16. N (M0) = 420, N (M1) = 78. *p < 0.05, **p < 0.01, ***p < 0.001.

with several immune and factors of six immune cells and factors (Figure 6H).

Functional Enrichment Analyses

GO and KEGG analyses were carried out for these 784 FI-DEGs between normal and patients with KIRC and 226 FI-DEGs between patients with KIRC with low-risk value and high-risk value (Supplementary Figure 4). There were 366 biological processes (BPs), 45 cellular components (CCs), 81 molecular functions (MFs), and 87 KEGG pathways that were enriched as measured by the False discovery rate (FDR) value <0.05 for those 784 FI-DEGs between the normal and patients with KIRC (Figures 7A, C and Supplementary Tables 3, 4). There were 68 BPs, 11 CCs, 18 MFs, and 16 KEGG pathways that were enriched as measured by the FDR value <0.05 for those 226 FI-

DEGs between patients with KIRC with low-risk value and high-risk value (Figures 7B, D and Supplementary Tables 5, 6).

Construction of the Diagnostic Model

A diagnostic model integrating these five DEGs (*CCR4*, *CMTM3*, *IFITM1*, *MX2*, and *NR3C2*) were established to separate KIRC from normal using a stepwise logistic regression method. Diagnostic scores were identified as follows: LOGIT score = 0.7998 + (0.1034)*Exp(*CMTM3*) + (-0.1590)*Exp(*NR3C2*) + (0.0465)*Exp(*MX2*) + (0.0737)*Exp(*CCR4*) + (0.0966)*Exp(*IFITM1*)

(Figure 8A). The LOGIT value of patients with KIRC was significantly higher than that of the normal (Figure 8B). The AUC value of the diagnostic model reached 0.9470 (Figure 8C). Correlation analyses indicated that these five FI-DEGs were significantly correlated the LOGIT value (Figure 8D). The

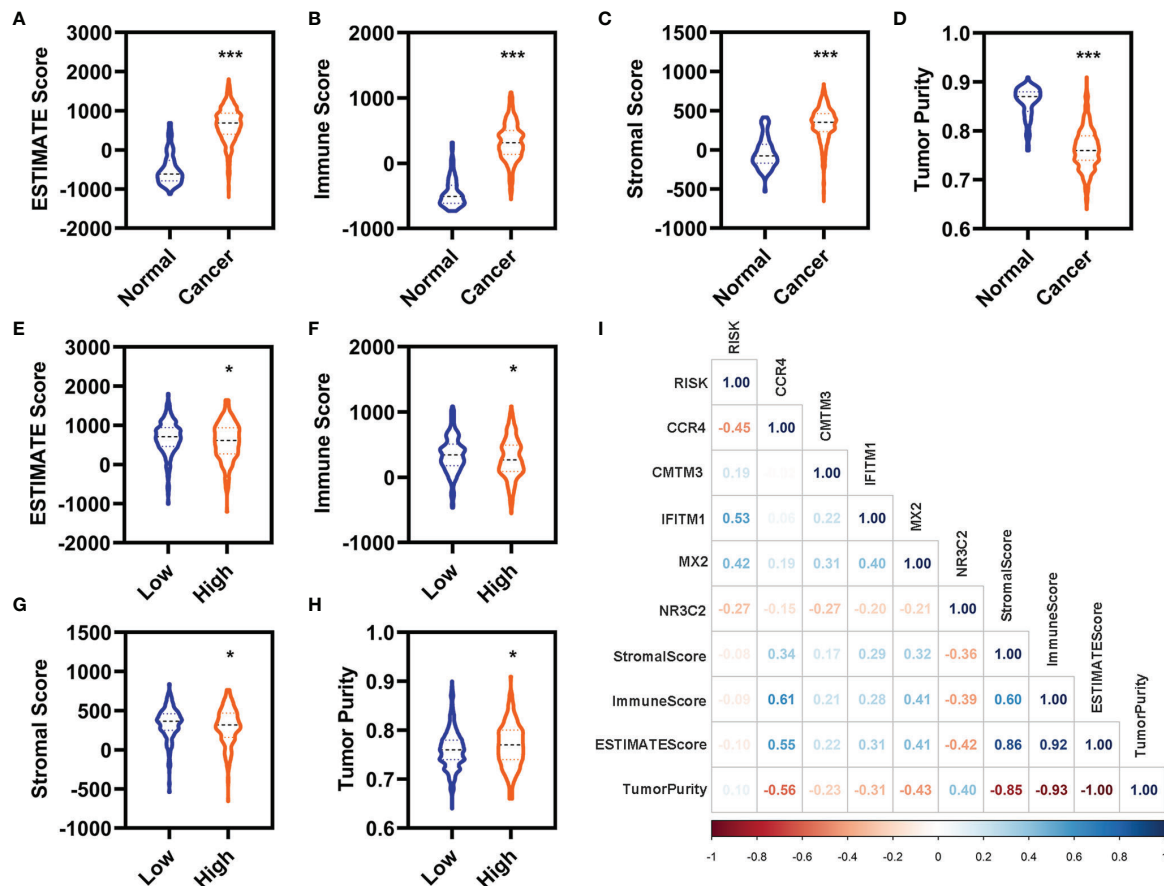


FIGURE 5 | Correlation analyses with the immune. (A–D) Differentially expressed analyses for the ESTIMATE (A), immune (B), stromal (C), and tumor purity (D) between the normal and patients with KIRC in the entire cohort. (E–H) Differentially expressed analyses for the ESTIMATE (E), immune (F), stromal (G), and tumor purity (H) between the patients with KIRC with low-risk value and high-risk value in the entire cohort. (I) Correlation analyses of these five FI-DEGs and risk value with the immune in the entire cohort. N (normal) = 72, N (cancer) = 530. N (low) = 336, N (high) = 194. *p < 0.05, ***p < 0.001.

sensitivity and specificity of the diagnostic model were 86.98% and 97.22%, respectively (Table 2).

DISCUSSIONS

DNA methylation is one of the most common epigenetic modifications, which plays important role in the regulation of the structure and expression of genes. Aberrant DNA methylations may lead to the inactivation of tumor suppressor genes or the activation of oncogenes, which could further lead to the cancerigenesis (9–11). Therefore, researchers have conducted a large number of studies related to the DNA methylation profile of various cancers. The DNA methylated profiles provide insights into the etiology of various cancers for the researcher and clinician in early diagnosis and precise treatment. In the present study, we aimed to identify suitable prognostic biomarkers related with aberrant methylations for KIRC using the TCGA data. We identified that FI-DEGs correlated with aberrant methylations (*CCR4*, *CMTM3*, *IFITM1*, *MX2*, and *NR3C2*) were significantly correlated with the OS of KIRC

independently. The prognostic model and diagnosis model constructed by these five FI-DEGs can be well used for the prognosis and diagnosis of KIRC respectively.

CCR4 (C-C Motif Chemokine Receptor 4) is the primary receptor for C-C motif chemokine ligand 17 and C-C motif chemokine ligand 22. Suppression of *CCR4* could suppress the migration, invasion, and proliferation for several cancers, such as lung cancer, breast cancer, and leukemia (32–34). Patients with high *CCR4* expression have a poorer survival prognosis (35). In the present study, we found that the expression of *CCR4* was significantly increased in the patients with KIRC. In addition, previous study also indicated that *CCR4* could be a prognostic biomarker and correlated with immune infiltrates in head and neck squamous cell carcinoma (36). *CCR4* could be used as a therapeutic target for cancer immunotherapy of several cancers, such as adult T-cell leukemia/lymphoma and cutaneous T-cell lymphomas (37). In our present study, we also found that *CCR4* was correlated with the infiltration of several immune cells and factors. However, what is very interesting was that patients with KIRC with high expression of *CCR4* displayed better OS. Therefore, we speculate that *CCR4* may only be related to the

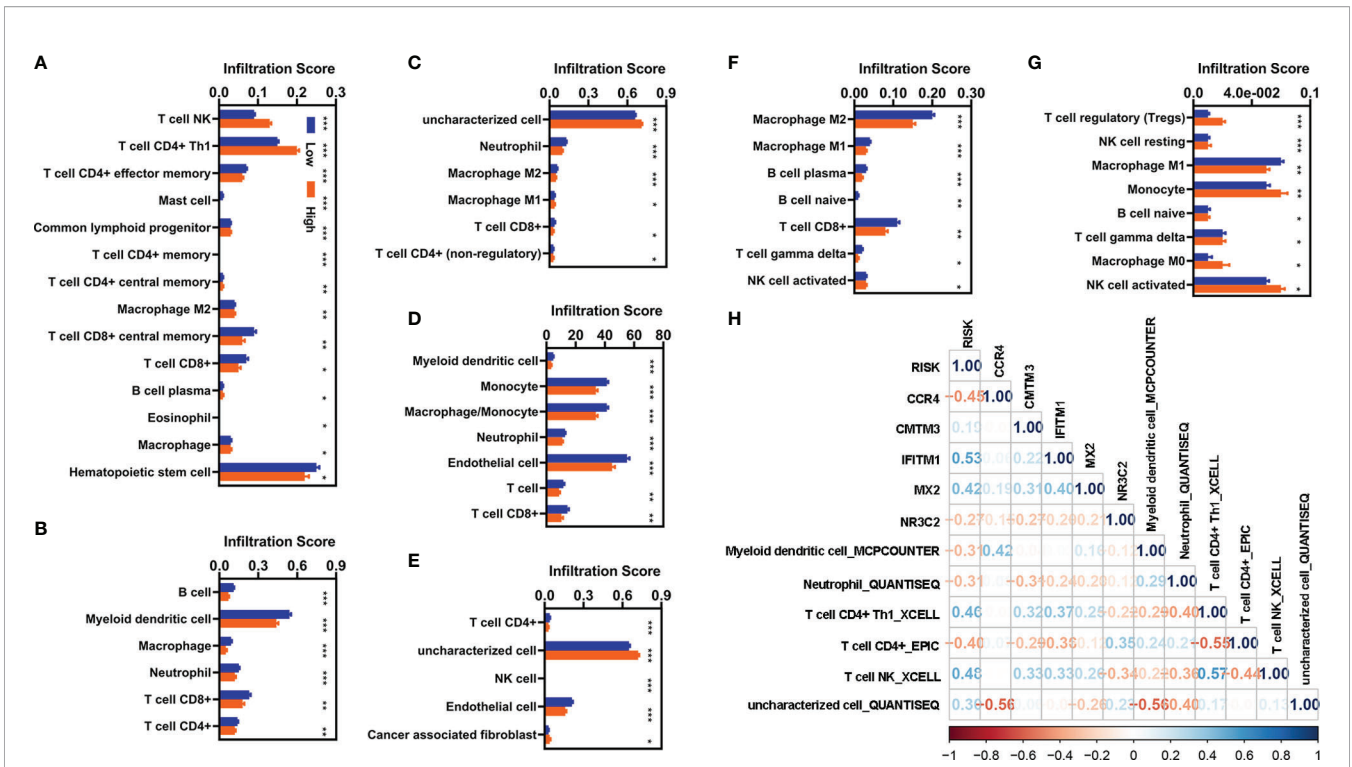


FIGURE 6 | Correlation analyses with the infiltration of immune cells and factors. (A–G) Differentially expressed analyses for infiltration of immune cells and factors with different risk value. (A) XCELL. (B) TIMER. (C) QUANTISEQ. (D) MCPOUNTER. (E) EPIC. (F) CIBERSORT-ABS. (G) CIBERSORT. (H) Correlation analyses of these five FI-DEGs and risk value with the immune cells and factors in the entire cohort. N (low) = 336, N (high) = 194. *p < 0.05, **p < 0.01, ***p < 0.001.

survival of KIRC and does not participate in the development of KIRC. CMTM3 (CKLF-like MARVEL transmembrane domain-containing 3), a member of the CMTM family, was found in several human tumors. In addition to being associated with immunity, CCR4 have also been implicated in iron death-related processes, such as Reactive oxygen species (ROS). Molinaro et al. found that Treg cells in *CCR4*^{-/-} sepsis mice showed reduced inhibition of ROS production by activated neutrophils (38). Hsu et al. found that CCR4 was involved in the regulation of ROS production by IL-20 (39). CMTM3 is closely connected with immune system and associated with sex during tumorigenesis (40). The expression of CMTM3 was decreased in several cancers, such as prostate cancer (41), and hepatic carcinoma (42). Overexpression of CMTM3 could inhibit the proliferation, migration, and invasion for several cancers (41, 42). However, the previous study also demonstrated that CMTM3 was overexpressed in pancreatic cancer (43). Results from the study of Zhou et al. indicated that CMTM3 could promote tumor aggressiveness in pancreatic cancer, and CMTM3 overexpression predicts poor survival (43). CMTM3 could be used as a potential prognostic biomarker of glioma, which is associated with immune invasion in the glioma microenvironment and may become a new immunotherapy target (44). In the present study, we also found that the expression of CMTM3 was increased. Patients with KIRC with high expression of CMTM3 displayed worse OS. All of these results indicated that CMTM3 may serve different role for

different cancers. IFITM1 (interferon-induced transmembrane protein 1) is a member of interferon stimulated family, which is expressed by T cells (45). Recent experiments have shown that IFITM protein is directly involved in adaptive immunity and regulates the differentiation of CD4⁺ T helper cells in a T-cell intrinsic manner (45). Results from the study of Lui et al. indicated that IFITM1 overexpression contributes to breast cancer progression (46). Yan et al. found that suppression of IFITM1 could suppress cell growth and metastasis for lung cancer (47). Numerous pieces of evidence indicated that IFITM1 may serve as prognostic biomarker due to the closely relationship with survival (48–50). Consistent with previous studies, we found that the expression of IFITM1 was increased and correlated with the OS of patients with KIRC. MX2 (MX dynamin-like GTPase 2) is a novel regulator of cell cycle in melanoma cells. Wang et al. found the overexpression of human MX2 gene suppresses cell proliferation, migration, and invasion. However, we found that MX2 was reduced in KIRC (51). It may be similar to CMTM3; MX2 may play different roles in different cancers. NR3C2 is nuclear receptor subfamily 3 group C member 2. Fan et al. found that the expression of NR3C2 was downregulated in breast cancer (52). High expression of NR3C2 was significantly correlated with prolonged OS (53). Overexpression NR3C2 could repress the proliferation, migration, and invasion for breast cancer and hepatocellular carcinoma (52, 54). Consistent with previous studies, NR3C2 was decreased in patients with KIRC. Moreover, low NR3C2

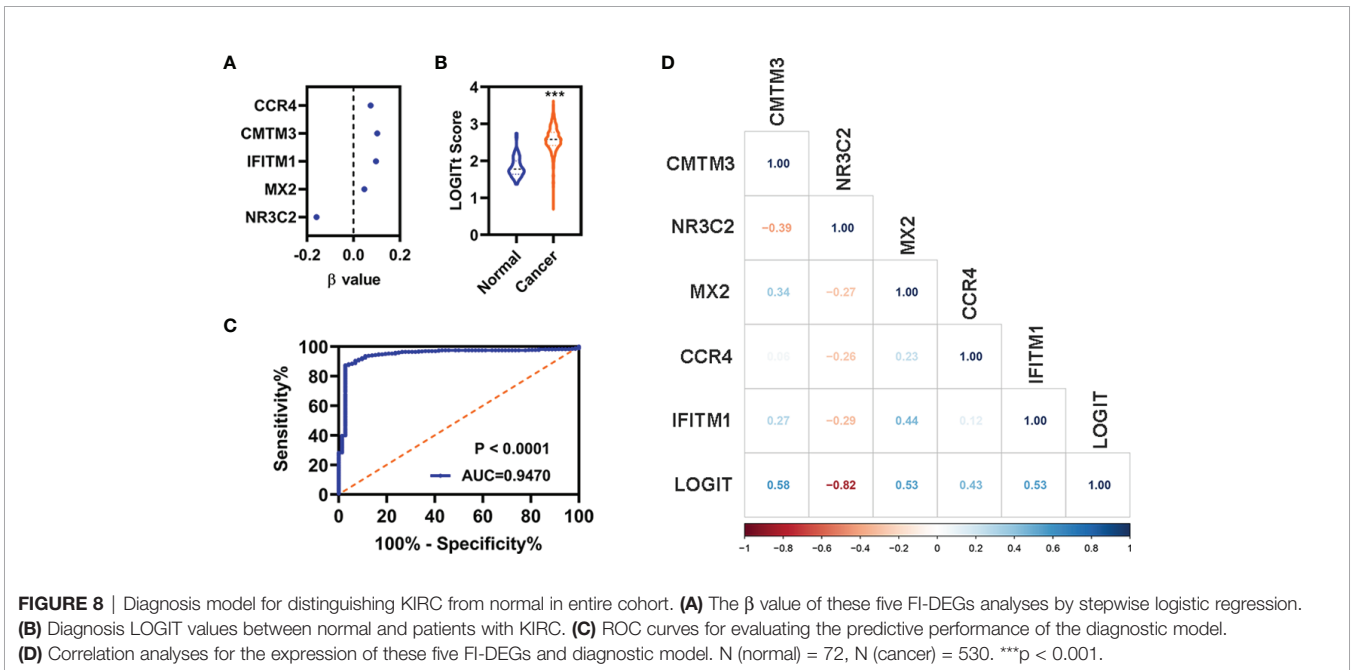
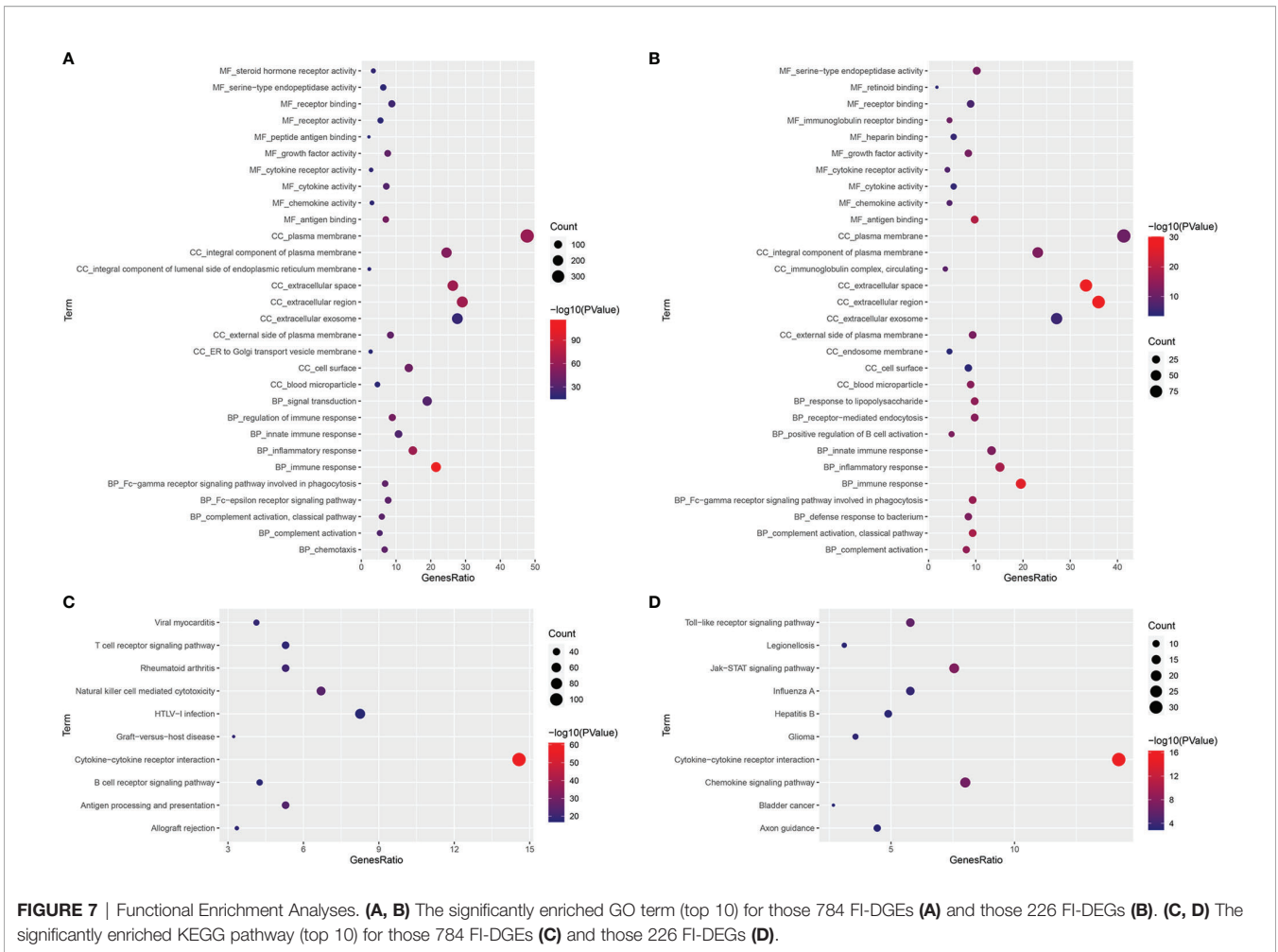


TABLE 2 | Sensitivity and specificity of diagnosis model.

	Real Cancer	Real Normal
Predicted Cancer	461	2
Predicted Normal	69	70
Total	530	72
Correct	461	70
Sensitivity	0.8698	
Specificity		0.9722

correlated with the metastasis and poor prognosis (55). Our studies reinforced the negative relationship of NR3C2 with the KIRC.

CONCLUSIONS

Our present data showed that the prognostic and diagnostic models using those five FI-DEGs (*CCR4*, *CMTM3*, *IFITM1*, *MX2*, and *NR3C2*) could well predict the outcome of patients with KIRC, which suggested that these five FI-DEGs could be used as prognosis and diagnosis biomarkers for KIRC. However, whether these five FI-DEGs are really associated with abnormal methylation and whether these five FI-DEGs can be used for clinical prognosis and diagnosis need further validation, especially clinical cross-validation.

REFERENCES

- Sung H, Ferlay J, Siegel RL, Laversanne M, Soerjomataram I, Jemal A, et al. Global Cancer Statistics 2020: GLOBOCAN Estimates of Incidence and Mortality Worldwide for 36 Cancers in 185 Countries. *CA Cancer J Clin* (2021) 71:209–49. doi: 10.3322/caac.21660
- Rini BI, Campbell SC, Escudier B. Renal Cell Carcinoma. *Lancet* (2009) 373:1119–32. doi: 10.1016/S0140-6736(09)60229-4
- Shuch B, Amin A, Armstrong AJ, Eble JN, Ficarra V, Lopez-Beltran A, et al. Understanding Pathologic Variants of Renal Cell Carcinoma: Distilling Therapeutic Opportunities From Biologic Complexity. *Eur Urol* (2015) 67:85–97. doi: 10.1016/j.eururo.2014.04.029
- Song J, Liu YD, Su J, Yuan D, Sun F, Zhu J. Systematic Analysis of Alternative Splicing Signature Unveils Prognostic Predictor for Kidney Renal Clear Cell Carcinoma. *J Cell Physiol* (2019) 234:22753–64. doi: 10.1002/jcp.28840
- Yin L, Li W, Wang G, Shi H, Wang K, Yang H, et al. NR1B2 Suppress Kidney Renal Clear Cell Carcinoma (KIRC) Progression by Regulation of LATS 1/2-YAP Signaling. *J Exp Clin Cancer Res* (2019) 38:343. doi: 10.1186/s13046-019-1344-3
- Hutson TE, Figlin RA. Renal Cell Cancer. *Cancer J* (2007) 13:282–6. doi: 10.1097/PPO.0b013e318156fe69
- Hsieh JJ, Purdue MP, Signoretti S, Swanton C, Albiges L, Schmidinger M, et al. Renal Cell Carcinoma. *Nat Rev Dis Primers* (2017) 3:17009. doi: 10.1038/nrdp.2017.9
- Gray RE, Harris GT. Renal Cell Carcinoma: Diagnosis and Management. *Am Fam Physician* (2019) 99:179–84.
- Dawson MA, Kouzarides T. Cancer Epigenetics: From Mechanism to Therapy. *Cell* (2012) 150:12–27. doi: 10.1016/j.cell.2012.06.013
- Amirghofran Z, Jalali SA, Hosseini SV, Vasei M, Sabayan B, Ghaderi A. Evaluation of CD44 and CD44v6 in Colorectal Carcinoma Patients: Soluble Forms in Relation to Tumor Tissue Expression and Metastasis. *J Gastrointest Cancer* (2008) 39:73–8. doi: 10.1007/s12029-009-9062-2
- Okugawa Y, Grady WM, Goel A. Epigenetic Alterations in Colorectal Cancer: Emerging Biomarkers. *Gastroenterology* (2015) 149:1204–1225:e1212. doi: 10.1053/j.gastro.2015.07.011

DATA AVAILABILITY STATEMENT

The data that support the findings of this study are openly available in TCGA at <https://portal.gdc.cancer.gov/>.

AUTHOR CONTRIBUTIONS

ZX and YZ conceived and designed the experiments. X-LX performed the analyses. YL, JL, HFZ, HRZ, QZ, PB, and TD helped to analyze the data. X-LX wrote the paper. All authors contributed to the article and approved the submitted version.

FUNDING

This project is financially supported by the Education Department of Hunan Province (20B417) and the Science and Technology Department of Huaihua (2020R3104).

SUPPLEMENTARY MATERIAL

The Supplementary Material for this article can be found online at: <https://www.frontiersin.org/articles/10.3389/fimmu.2022.851312/full#supplementary-material>

- Klutstein M, Nejman D, Greenfield R, Cedar H. DNA Methylation in Cancer and Aging. *Cancer Res* (2016) 76:3446–50. doi: 10.1158/0008-5472.CAN-15-3278
- Toh TB, Lim JJ, Chow EK. Epigenetics in Cancer Stem Cells. *Mol Cancer* (2017) 16:29. doi: 10.1186/s12943-017-0596-9
- Ayob AZ, Ramasamy TS. Cancer Stem Cells as Key Drivers of Tumour Progression. *J BioMed Sci* (2018) 25:20. doi: 10.1186/s12929-018-0426-4
- Broske AM, Vockentanz L, Kharazi S, Huska MR, Mancini E, Scheller M, et al. DNA Methylation Protects Hematopoietic Stem Cell Multipotency From Myeloerythroid Restriction. *Nat Genet* (2009) 41:1207–15. doi: 10.1038/ng.463
- Morita R, Hirohashi Y, Suzuki H, Takahashi A, Tamura Y, Kanaseki T, et al. DNA Methyltransferase 1 is Essential for Initiation of the Colon Cancers. *Exp Mol Pathol* (2013) 94:322–9. doi: 10.1016/j.yexmp.2012.10.004
- Liu CC, Lin JH, Hsu TW, Su K, Li AF, Hsu HS, et al. IL-6 Enriched Lung Cancer Stem-Like Cell Population by Inhibition of Cell Cycle Regulators via DNMT1 Upregulation. *Int J Cancer* (2015) 136:547–59. doi: 10.1002/ijc.29033
- Joosten SC, Smits KM, Aarts MJ, Melotte V, Koch A, Tjan-Heijnen VC, et al. Epigenetics in Renal Cell Cancer: Mechanisms and Clinical Applications. *Nat Rev Urol* (2018) 15:430–51. doi: 10.1038/s41585-018-0023-z
- Klumper N, Ralser DJ, Bawden EG, Landsberg J, Zarbl R, Kristiansen G, et al. LAG3 (LAG-3, CD223) DNA Methylation Correlates With LAG3 Expression by Tumor and Immune Cells, Immune Cell Infiltration, and Overall Survival in Clear Cell Renal Cell Carcinoma. *J Immunother Cancer* (2020) 8:e000552. doi: 10.1136/jitc-2020-000552
- Matsushita M, Freigang S, Schneider C, Conrad M, Bornkamm GW, Kopf M. T Cell Lipid Peroxidation Induces Ferroptosis and Prevents Immunity to Infection. *J Exp Med* (2015) 212:555–68. doi: 10.1084/jem.20140857
- Wang D, Dubois RN. Immunosuppression Associated With Chronic Inflammation in the Tumor Microenvironment. *Carcinogenesis* (2015) 36:1085–93. doi: 10.1093/carcin/bgv123
- Wang D, Xie N, Gao W, Kang R, Tang D. The Ferroptosis Inducer Erastin Promotes Proliferation and Differentiation in Human Peripheral Blood Mononuclear Cells. *Biochem Biophys Res Commun* (2018) 503:1689–95. doi: 10.1016/j.bbrc.2018.07.100

23. Stockwell BR, Jiang X. A Physiological Function for Ferroptosis in Tumor Suppression by the Immune System. *Cell Metab* (2019) 30:14–5. doi: 10.1016/j.cmet.2019.06.012
24. Wang W, Green M, Choi JE, Gijon M, Kennedy PD, Johnson JK, et al. CD8(+) T Cells Regulate Tumour Ferroptosis During Cancer Immunotherapy. *Nature* (2019) 569:270–4. doi: 10.1038/s41586-019-1170-y
25. Li Z, Rong L. Cascade Reaction-Mediated Efficient Ferroptosis Synergizes With Immunomodulation for High-Performance Cancer Therapy. *Biomater Sci* (2020) 8:6272–85. doi: 10.1039/D0BM01168A
26. Hassanna B, Vandenabeele P, Vanden Berghe T. Targeting Ferroptosis to Iron Out Cancer. *Cancer Cell* (2019) 35:830–49. doi: 10.1016/j.ccell.2019.04.002
27. Zou Y, Palte MJ, Deik AA, Li H, Eaton JK, Wang W, et al. A GPX4-Dependent Cancer Cell State Underlies the Clear-Cell Morphology and Confers Sensitivity to Ferroptosis. *Nat Commun* (2019) 10:1617. doi: 10.1038/s41467-019-09277-9
28. Galluzzi L, Humeau J, Buque A, Zitvogel L, Kroemer G. Immunostimulation With Chemotherapy in the Era of Immune Checkpoint Inhibitors. *Nat Rev Clin Oncol* (2020) 17:725–41. doi: 10.1038/s41571-020-0413-z
29. Yi J, Zhu J, Wu J, Thompson CB, Jiang X. Oncogenic Activation of PI3K-AKT-mTOR Signaling Suppresses Ferroptosis via SREBP-Mediated Lipogenesis. *Proc Natl Acad Sci USA* (2020) 117:31189–97. doi: 10.1073/pnas.2017152117
30. Fan CN, Ma L, Liu N. Systematic Analysis of lncRNA-miRNA-mRNA Competing Endogenous RNA Network Identifies four-lncRNA Signature as a Prognostic Biomarker for Breast Cancer. *J Transl Med* (2018) 16:264. doi: 10.1186/s12967-018-1640-2
31. Xing XL, Xing C, Huang Z, Yao ZY, Liu YW. Immune-Related lncRNAs to Construct Novel Signatures and Predict the Prognosis of Rectal Cancer. *Front Oncol* (2021) 11:661846. doi: 10.3389/fonc.2021.661846
32. Li JY, Ou ZL, Yu SJ, Gu XL, Yang C, Chen AX, et al. The Chemokine Receptor CCR4 Promotes Tumor Growth and Lung Metastasis in Breast Cancer. *Breast Cancer Res Treat* (2012) 131:837–48. doi: 10.1007/s10549-011-1502-6
33. Liu LB, Xie F, Chang KK, Shang WQ, Meng YH, Yu JJ, et al. Chemokine CCL17 Induced by Hypoxia Promotes the Proliferation of Cervical Cancer Cell. *Am J Cancer Res* (2015) 5:3072–84.
34. Hu J, Wang L, Guan C. MiR-532-5p Suppresses Migration and Invasion of Lung Cancer Cells Through Inhibiting Ccr4. *Cancer Biother Radioph* (2020) 35:673–81. doi: 10.1089/cbr.2019.3258
35. Shono Y, Suga H, Kamijo H, Fujii H, Oka T, Miyagaki T, et al. Expression of CCR3 and CCR4 Suggests a Poor Prognosis in Mycosis Fungoides and Sezary Syndrome. *Acta Derm Venereol* (2019) 99:809–12. doi: 10.2340/00015555-3207
36. Zhang Y, Chen K, Li L, Mao W, Shen D, Yao N, et al. CCR4 is a Prognostic Biomarker and Correlated With Immune Infiltrates in Head and Neck Squamous Cell Carcinoma. *Ann Transl Med* (2021) 9:1443. doi: 10.21037/atm-21-3936
37. Yoshie O. CCR4 as a Therapeutic Target for Cancer Immunotherapy. *Cancers (Basel)* (2021) 13:5542. doi: 10.3390/cancers13215542
38. Molinaro R, Pecli C, Guilherme RF, Alves-Filho JC, Cunha FQ, Canetti C, et al. CCR4 Controls the Suppressive Effects of Regulatory T Cells on Early and Late Events During Severe Sepsis. *PLoS One* (2015) 10:e0133227. doi: 10.1371/journal.pone.0133227
39. Hsu YH, Wei CC, Shieh DB, Chan CH, Chang MS. Anti-IL-20 Monoclonal Antibody Alleviates Inflammation in Oral Cancer and Suppresses Tumor Growth. *Mol Cancer Res* (2012) 10:1430–9. doi: 10.1158/1541-7786.MCR-12-0276
40. Hu FZ, Sheng ZZ, Qin CP, Xu T. Research Advances in CKLF-like MARVEL Transmembrane Domain Containing Member 3. *Zhongguo Yi Xue Ke Xue Yuan Xue Bao* (2016) 38:360–3.
41. Hu F, Yuan W, Wang X, Sheng Z, Yuan Y, Qin C, et al. CMTM3 is Reduced in Prostate Cancer and Inhibits Migration, Invasion and Growth of LNCaP Cells. *Clin Transl Oncol* (2015) 17:632–9. doi: 10.1007/s12094-015-1288-9
42. Li W, Zhang S. CKLF-Like MARVEL Transmembrane Domain-Containing Member 3 (CMTM3) Inhibits the Proliferation and Tumorigenesis in Hepatocellular Carcinoma Cells. *Oncol Res* (2017) 25:285–93. doi: 10.3727/096504016X14732523471442
43. Zhou Z, Ma Z, Li Z, Zhuang H, Liu C, Gong Y, et al. CMTM3 Overexpression Predicts Poor Survival and Promotes Proliferation and Migration in Pancreatic Cancer. *J Cancer* (2021) 12:5797–806. doi: 10.7150/jca.57082
44. Li S, Gao P, Dai X, Ye L, Wang Z, Cheng H. New Prognostic Biomarker CMTM3 in Low Grade Glioma and its Immune Infiltration. *Ann Transl Med* (2022) 10:206. doi: 10.21037/atm-22-526
45. Yanez DC, Ross S, Crompton T. The IFITM Protein Family in Adaptive Immunity. *Immunology* (2020) 159:365–72. doi: 10.1111/imm.13163
46. Lui AJ, Geanes ES, Ogony J, Behbod F, Marquess J, Valdez K, et al. IFITM1 Suppression Blocks Proliferation and Invasion of Aromatase Inhibitor-Resistant Breast Cancer *In Vivo* by JAK/STAT-Mediated Induction of P21. *Cancer Lett* (2017) 399:29–43. doi: 10.1016/j.canlet.2017.04.005
47. Yan J, Jiang Y, Lu J, Wu J, Zhang M. Inhibiting of Proliferation, Migration, and Invasion in Lung Cancer Induced by Silencing Interferon-Induced Transmembrane Protein 1 (Ifitm1). *BioMed Res Int* (2019) 2019:9085435. doi: 10.1155/2019/9085435
48. Borg D, Hedner C, Gaber A, Nodin B, Fristedt R, Jirstrom K, et al. Expression of IFITM1 as a Prognostic Biomarker in Resected Gastric and Esophageal Adenocarcinoma. *biomark Res* (2016) 4:10. doi: 10.1186/s40364-016-0064-5
49. Koh YW, Han JH, Jeong D, Kim CJ. Prognostic Significance of IFITM1 Expression and Correlation With Microvessel Density and Epithelial-Mesenchymal Transition Signature in Lung Adenocarcinoma. *Pathol Res Pract* (2019) 215:152444. doi: 10.1016/j.prp.2019.152444
50. Li D, Yang Z, Liu Z, Zou Q, Yuan Y. DDR2 and IFITM1 Are Prognostic Markers in Gallbladder Squamous Cell/Adenosquamous Carcinomas and Adenocarcinomas. *Pathol Oncol Res* (2019) 25:157–67. doi: 10.1007/s12253-017-0314-3
51. Wang H, Guan Q, Nan Y, Ma Q, Zhong Y. Overexpression of Human MX2 Gene Suppresses Cell Proliferation, Migration, and Invasion via ERK/P38/NF-kappaB Pathway in Glioblastoma Cells. *J Cell Biochem* (2019) 120:18762–70. doi: 10.1002/jcb.29189
52. Fan Y, Li Y, Zhu Y, Dai G, Wu D, Gao Z, et al. miR-301b-3p Regulates Breast Cancer Cell Proliferation, Migration, and Invasion by Targeting Nr3c2. *J Oncol* (2021) 2021:8810517. doi: 10.1155/2021/8810517
53. Lu J, Hu F, Zhou Y. NR3C2-Related Transcriptome Profile and Clinical Outcome in Invasive Breast Carcinoma. *BioMed Res Int* (2021) 2021:9025481. doi: 10.1155/2021/9025481
54. Yang C, Ma X, Guan G, Liu H, Yang Y, Niu Q, et al. MicroRNA-766 Promotes Cancer Progression by Targeting NR3C2 in Hepatocellular Carcinoma. *FASEB J* (2019) 33:1456–67. doi: 10.1096/fj.201801151R
55. Zhao Z, Zhang M, Duan X, Deng T, Qiu H, Zeng G. Low NR3C2 Levels Correlate With Aggressive Features and Poor Prognosis in non-Distant Metastatic Clear-Cell Renal Cell Carcinoma. *J Cell Physiol* (2018) 233:6825–38. doi: 10.1002/jcp.26550

Conflict of Interest: The authors declare that the research was conducted in the absence of any commercial or financial relationships that could be construed as a potential conflict of interest.

Publisher's Note: All claims expressed in this article are solely those of the authors and do not necessarily represent those of their affiliated organizations, or those of the publisher, the editors and the reviewers. Any product that may be evaluated in this article, or claim that may be made by its manufacturer, is not guaranteed or endorsed by the publisher.

Copyright © 2022 Xing, Liu, Liu, Zhou, Zhang, Zuo, Bu, Duan, Zhou and Xiao. This is an open-access article distributed under the terms of the Creative Commons Attribution License (CC BY). The use, distribution or reproduction in other forums is permitted, provided the original author(s) and the copyright owner(s) are credited and that the original publication in this journal is cited, in accordance with accepted academic practice. No use, distribution or reproduction is permitted which does not comply with these terms.